ISSN 1392–1320 MATERIALS SCIENCE (MEDŽIAGOTYRA). Vol. 20, No. 1. 2014

Effect of Sol-Gel Ageing Time on Three Dimensionally Ordered Macroporous Structure of $80SiO_2$-$15CaO$-$5P_2O_5$ Bioactive Glasses

Thanida CHAROENSUK [1], Upsorn BOONYANG [1], Chitnarong SIRISATHITKUL [1 *], Pornsak PANCHAWIRAT [2], Payoon SENTHONGKAEW [3]

[1] *Molecular Technology Research Unit, School of Science, Walailak University, 222 Thaiburi, Nakhon Si Thammarat, 80161, Thailand*
[2] *Thailand Center of Excellence in Physics, CHE, 328 Si Ayutthaya Rd., Bangkok, 10400, Thailand*
[3] *Department of Materials Engineering, Faculty of Engineering, Kasetsart University, 50 Ngam Wong Wan Rd., Bangkok, 10900, Thailand*

crossref http://dx.doi.org/10.5755/j01.ms.20.1.4755

Received 08 July 2013; accepted 29 September 2013

Three dimensionally ordered macroporous bioactive glasses (3DOM-BGs), namely $80SiO_2$-$15CaO$-$5P_2O_5$, were synthesized by sol-gel method. PMMA colloidal crystals and non-ionic block copolymers P123 were used as cotemplates. The amorphous 3DOM-BGs had skeletal walls enclosing macropores. Such structure resulted from octahedral and tetrahedral holes of the face-centered cubic (*fcc*) closest packed PMMA templates and windows interconnecting through macropores network. The thicknesses of the walls were around 50 nm – 80 nm and the windows were 90 nm – 110 nm in diameter. These wall thickness is increased by with an increase in ageing time up to 24 h and then gradually reduced with further increase in aging time. Vibration bands of Si–O–Si and P–O were evident in infrared spectra which are in agreement with EDS spectra indicating Si, P and Ca compositions. After *in vitro* bioactivity testing by soaking 3DOM-BGs in simulated body fluid at 37 °C, the crystallization of amorphous calcium phosphate layers compatible to the bone component of hydroxyl carbonate apatite were rapidly formed within 3 h. These results indicated that these 3DOM-BGs resembled ideal bone implant materials.
Keywords: three dimensionally ordered macroporous bioactive glass, sol-gel method, *in vitro* testing.

1. INTRODUCTION

Bioactive glasses were first successfully produced from $45wt\%SiO_2$-$24.5wt\%CaO$-$24.5wt\%Na_2O$-$6wt\%P_2O_5$ by the melt-quenching method and referred to as 45S5 Bioglass® by Hench et al [1]. Since then, various kinds of bioactive glasses have been extensively developed and used in clinical applications as implanted biomaterials to replace or regenerate bone defects. They commonly consist of the silicate network incorporating calcium, sodium, and phosphorus in specific compositions. In some cases, the silicate network may include only calcium and phosphorus, or additional elements such as magnesium, potassium, iron, silver, or zinc to functionalize in certain applications. The key compositions for bioactivity of bioactive glasses are approximately (30 – 55) wt% of SiO_2, (15 – 30) wt% of CaO, (20 – 25) wt% of Na_2O, and (4 – 7) wt% of P_2O_5 [2]. The bone-bonding ability of these bioactive glasses is determined from the biodegradable, the dissolution rate of ions when exposed to physiological fluids, the formation of new bones and stimulation of osteoblast. The mechanism of bone-bonding was suggested by Hench et al. [1]. Initially, the network modifications of Ca^{2+} and Na^+ ions at the interface of glass are dissolved and replaced by H^+ in the body fluid. As a result, the increase in pH which promotes the breaking of siloxane groups (Si–O–Si) releases some soluble silica and silanol groups (Si–OH) at the surface are developed. The silica-rich surface layer then condense and repolymerise to form the amorphous calcium silicate layer. By incorporating PO_4^{3-} and Ca^{2+} ions from the body fluid, the amorphous calcium phosphate layer is formed. Finally, hydroxyl carbonate apatite (HCA) is biologically crystallized leading to the formation of new tissue by interaction with other biomolecules and cells.

Recently, the sol-gel method has increasingly been employed as an alternative to the traditional high temperature techniques [2 – 4]. A variety compositions were obtained in sol-gel derived bioactive glasses [5 – 9]. More importantly, the sol-gel method can incorporate the template for the growth of Three Dimensionally Ordered Macroporous Bioactive Glasses (3DOM-BGs). The versatility of such porous structures with a high surface-to-volume ratio is already exploited in the bone regenerations [10 – 12]. By virtue of the finite size effects [13], physical properties of these 3DOM-BGs structures were dependent on size and shape of windows interconnecting macropores and thickness of walls. Moreover, 3DOM structures tend to collapse if their walls are too thin as a result of the shrinkage effect in the polycondensation reaction to form gel.

In this work, 3DOM-BGs were synthesized using sol-gel method with monodispersed spherical poly-methly methacrylate (PMMA) colloidal crystals as macroporous templates. PMMA templates have been successfully employed in a variety of 3DOM structures [14, 15]. With a uniform size of PMMA templates, the wall thicknesess of 3DOM-BGs were by varying the period of ageing from sol to gel. The bioactivity of these 3DOM-BGs was then investigated to find the appropriate wall thickness.

* Corresponding author. Tel.: +6675-672945, fax: +6675-672004.
E-mail address: *chitnarong.siri@gmail.com* (C. Sirisathitkul)

2. MATERIALS AND METHOD

The compositions and details of starting materials are listed in Table 1. Tetraethyl orthosilicate (TEOS), calcium nitrate tetrahydrate ($Ca(NO_3)_2{\cdot}4H_2O$), triethyl phosphate (TEP), P123 (EO_{20}-PO_{70}-EO_{20}), ethanol (C_2H_5OH), and hydrochloric acid (HCl) were successively mixed together. The solution was vigorously stirred at room temperature by the magnetic stirrer to obtain a clear sol (hydrolysis reaction) and further stirred to reach the gel point (condensation reaction) [2, 11, 16]. To obtain 3DOM structure, PMMA colloidal crystals (sphere diameter is 350 nm) were completely immersed in this sol. The excess solution was removed. The products were then aged in the sealed vials at 60 °C with varying ageing time as 0, 12, 24, 36, 48, 60, 72 h. Afterwards, the samples were dried at 60 °C to eliminate excess solvents, catalysts and by-products for at least 24 h. Finally, the dried samples were calcined at 600 °C for 6 h (heating rate 2 °C/min, cooling rate 20 °C/min) to remove the cotemplates.

Table 1. Chemicals used in the synthesis of $80SiO_2$-15CaO--$5P_2O_5$ 3DOM-BGs

Reagents	Compositions	Amount
$C_8H_{20}O_4Si$ (TEOS)	80 %mole SiO_2	8.93 ml
$Ca(NO_3)_2{\cdot}4H_2O$	15 %mole CaO	1.77 g
$C_6H_{15}O_4P$ (TEP)	5 %mole P_2O_5	0.76 ml
$(C_3H_6O{\cdot}C_2H_4O)_x$(P123)		3.33 g
C_2H_5OH		12.50 ml
0.5M HCl		5.00 ml
PMMA		

Field emission scanning electron microscope (FESEM; JEOL JSM-7001F) operated at 5 kV – 20 kV was used to characterize the morphology of 3DOM-BGs providing details of structure, size and shape of skeleton walls and windows between macropores. Moreover, the surface change of 3DOM-BGs after *in vitro* bioactivity test can also be tracked. All samples were coated by conductive layers to prevent charge accumulation. Additionally, the 3DOM-BGs compositions were analyzed by the energy dispersive spectrometry (EDS; OXFORD PentaFETx3) attached to the FESEM with Silicon (Lithium drifted) crystal detectors. The X-ray diffraction (XRD; Philips X'Pert) using CuK_α radiation with a step 2°/min in the range 10° – 70° was used to identify phase present in 3DOM-BGs both before and after *in vitro* bioactivity test. The Fourier transform infrared spectroscopy (FT-IR; BRUKER Tensor27) was carried out in the transmission mode with a mid-infrared range 400 cm^{-1} – 4000 cm^{-1} at the resolution of 4 cm^{-1}. The samples were prepared in forms of KBr-based pellets. Functional groups of 3DOM-BGs both before and after *in vitro* bioactivity test can be verified.

The simulated body fluid (SBF) solution was prepared from reagents given in Table 2. They were completely dissolved one by one in 750 ml deionized water at 37 °C. $(CH_2OH)_3CNH_2$ was slowly added and the pH was adjusted to 7.25 by HCl. After that, 1000 ml of solution was kept in a volumetric flask until its temperature was down to a room temperature. The SBF solution was then stored in refrigerator. For the test, the solution is without precipitations and its storage time does not exceed 1 month.

Table 2. Amount of reagents for preparation 1000 ml of SBF, pH 7.25

Reagents		Amount
NaCl	Assay min. 100.0 %	7.996 g
$NaHCO_3$	Assay min. 100.3 %	0.350 g
KCl	Assay min. 100.1 %	0.224 g
K_2HPO_4	Assay min. 99.7 %	0.174 g
$MgCl_2{\cdot}6H_2O$	Assay min. 99.8 %	0.305 g
1M HCl	87.28 mL	40 cm^3
$CaCl_2{\cdot}2H_2O$	Assay min. 99.8 %	0.369 g
Na_2SO_4		0.071 g
$(CH_2OH)_3CNH_2$	Assay min. 99.9+ %	6.057 g
1M HCl	See above	Appropriate amount for adjusting pH

The *in vitro* bioactivity of 3DOM-BGs was tested at body temperature of 37 °C by using the SBF solution whose composition and ionic concentration similar to human blood plasma. Following Kokubo method [17], the grainy 3DOM-BGs were soaked in the SBF solution at 37 ºC for 3, 6, 12, 24, 48 and 72 h with daily refreshing of the SBF solution. After soaking, samples were removed from the SBF solution and washed with deionized water several times and air-dried at room temperature. The changes in 3DOM-BGs were monitored by FESEM, XRD and FTIR techniques. Hydroxyl carbonate apatite (HCA) formation has been recognized as a testament to the biological compatibility of bioactive materials [18, 19].

3. RESULTS AND DISCUSSION

All samples exemplified in Fig. 1 appear glitter in the primary observation with unaided eyes due to their porous structure. The sample without ageing (0 h) is brittle.

a b c

Fig. 1. Photographs of PMMA colloidal crystals (a) and 3DOM--BGs obtained after 0 h (b) and 48 h (c) ageing

Three-dimensional scaffolds in 3DOM-BGs are inherited from PMMA structure via colloidal crystal templates (CCT) method [20]. With infiltration technique, sol penetrated into the octahedral and tetrahedral holes of the closed-pack face-centered cubic (fcc) structure of spherical PMMA colloidal crystals used as macroporous templates. By the polycondensation reaction during ageing, sol turns into gel and the gel network then is expanded by the polymerization process [2, 11]. After the gel is dried, the solid already fills in interstitial spaces of templates. By calcination at 600 °C to obtain bioactive glass, the PMMA colloidal crystals were removed opening up macropore spaces and windows between macropores. The remaining

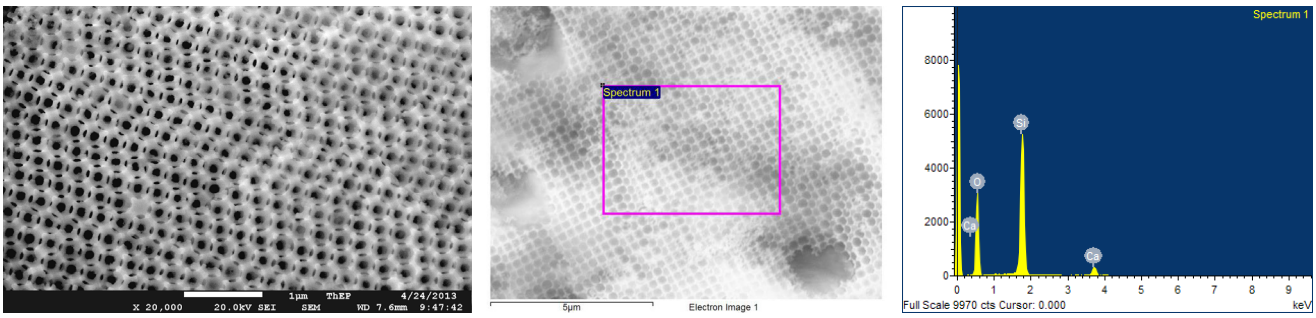

a b c

Fig. 2. FESEM image of 3DOM-BGs aged for 48 h (a) with a selected area (b) and corresponding EDS spectrum (c)

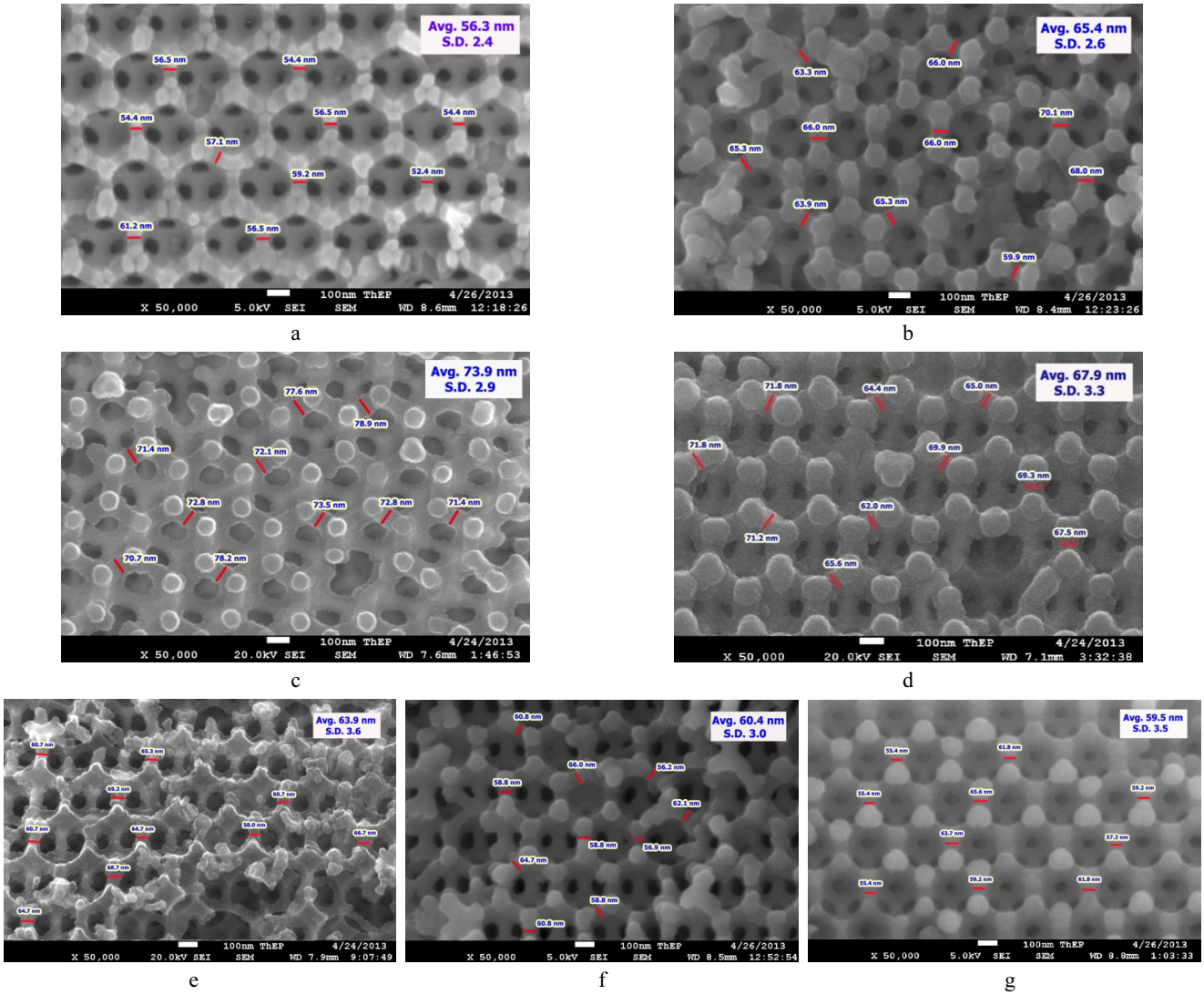

a b c d e f g

Fig. 3. Plane view FESEM images of 3DOM-BGs with the measurement of wall thickness. Sol-gel ageing times are: a – 0, b – 12, c – 24, d – 36, e – 48, f – 60 and g – 72 h

solid skeleton encloses the air holes leading to the 3DOM-BGs scaffolds as shown in Fig. 2. The peaks in EDS spectrum correspond to Si, Ca, O without impurity element. Since the intensity in EDS peaks is related to the elemental composition, P with the smallest fraction is not detected. The P peak was barely registered in the other work with comparable compositions [20] but was clearly shown in when the P_2O_5 was approximately doubled [21]. However, the subsequent analysis of FTIR indicates that the element P is a composition of 3DOM-BGs. The skeletal walls enclose macropores interconnected through windows positioned at touched point of spherical PMMA colloidal crystals. Regardless of template and precursor types, differences in size and shape of windows interconnecting macropores and thickness of walls are affected by the shrinkage of the precursor or the template. Moreover, the diameter of macropores is typically reduced by 10 %–30 % [22]. According to significant shrinkage of the gel due to the polycondensation reaction during ageing time, FESEM images of seven samples with varying ageing times from 0 h–72 h were compared in Fig. 3. The thicknesses from ten positions of skeletal walls for each sample were measured to

obtain an average value. The average wall thickness ranges from 56 nm to 74 nm within the standard deviation of 2.4 nm – 3.6 nm. The ageing time plotted against the average of thickness of walls in Fig. 4 show the effect of ageing time on the skeletal walls. The wall thickness is increased with longer ageing up to 24 h and then gradually reduced with further increases in ageing time. It implies that the polycondensation and polymerization are not complete during the first 24 h of ageing process and the shrinkage occurs after complete gelation.

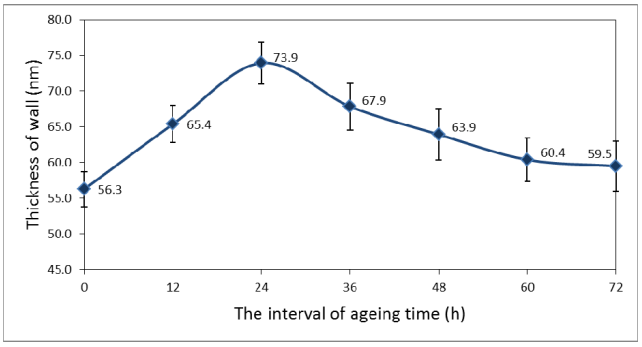

Fig. 4. Sol-gel ageing time plotted against the thickness of 3DOM-BG walls

FESEM images in Fig. 5 evidently start to form bone-like apatite of 3DOM-BGs after soaking in SBF solutions for only 3 h. There are marked differences in the formation rate of the bone-like apatite crystalline phase as confirmed by XRD and FTIR. Moreover, this crystalline phase is increased on the surface of 3DOM-BGs with increasing soaking time.

XRD spectra in Fig.6 indicate the amorphous state of 3DOM-BGs aged for 24 h and 72 h prior to the soaking in SBF solutions. The crystalline phase of HCA, the major inorganic component of bone [18, 19, 23], is detected on surface of both samples after soaking. For 48 h soaking, the diffraction peaks at 21.8, 22.9, 25.9, 28.1, 28.9, 31.8, 32.2, 32.9, 34.1, 46.7, 48.6 and 49.4 degree are assigned to the crystalline HCA phase (JCPDS 009-0432) in the 3DOM-BG aged for 24 h. However, the 3DOM-BG aged for 72 h exhibits only some diffraction peaks that idexed as HCA at 21.8, 22.9, 25.9 and 31.8 degree (JCPDS 009-0432). Moreover, a comparison of these spectra reveals that the peaks of 3DOM-BG aged for 24 h are sharper than those from 72 h ageing. In addition to the biological compatibility of these synthesized 3DOM-BGs, the results also show the potentially rapid growth in 3DOM-BG by using 24 h over the 72 h ageing counterpart.

In Fig. 7, FTIR spectra confirm the evolution of HCA layer on surface of 3DOM-BGs in both samples. Before soaking in SBF, both similar spectra show the peak at 466, 802 and 1090 cm^{-1} and shoulder between (1090 – 1220) cm^{-1} relate to Si–O–Si and 564 cm^{-1} relate to P–O vibrational bands. In addition, the vibrational bands of the carbonate groups can be observed at 1430 cm^{-1} and 1484 cm^{-1}. After soaking in SBF, the peaks that relate to Si-O-Si are weaken according to the breaking of siloxane group due to the mechanism to form HCA [1]. The vibrational peak of P–O near 564 cm^{-1} split to dual peaks at 564 cm^{-1} and 603 cm^{-1} and the peak at 960 cm^{-1} can be observed after soaking in SBF for 3 h. Furthermore, the intensity of vibrational peak of P–O is increased with the increase in soaking time. These results indicate the crystallization of amorphous phosphate related to the formation of HCA.

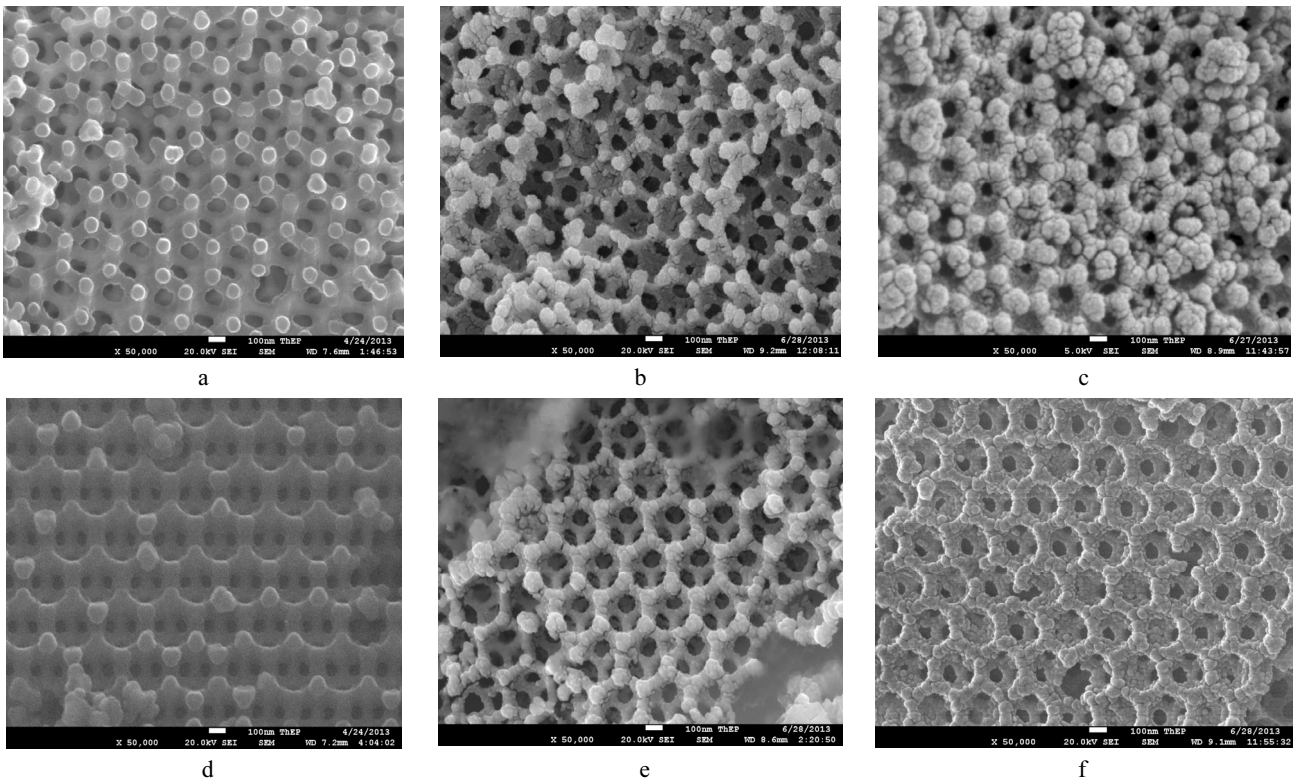

Fig. 5. FESEM images of 3DOM-BGs at 24 h and 72 h ageing (a, d) before soaking and (b, e) 3 h and (c, f) 6 h after soaking in SBF solution, respectively

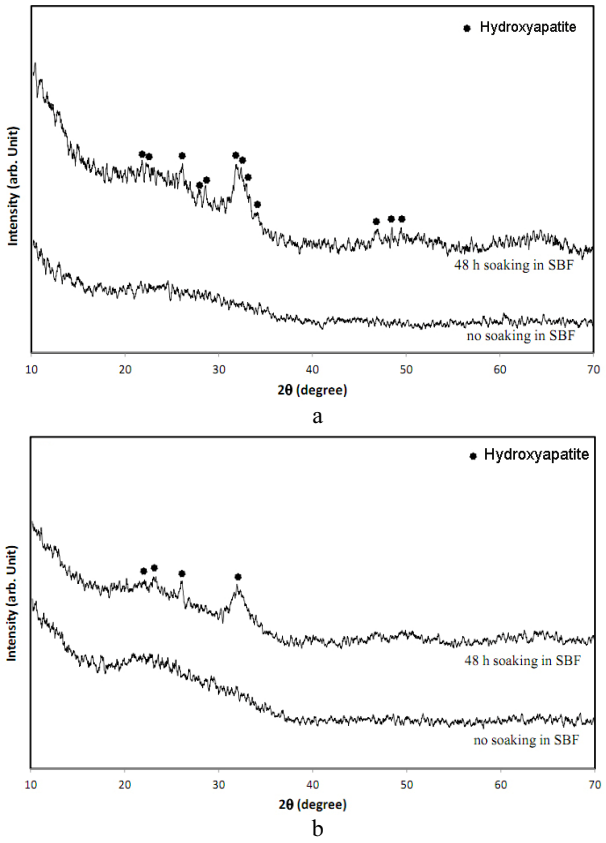

Fig. 6. Comparison of XRD spectra of 3DOM-BGs aged for 24 h (a) and 72 h (b), before and after soaking in SBF solutions for 48 h

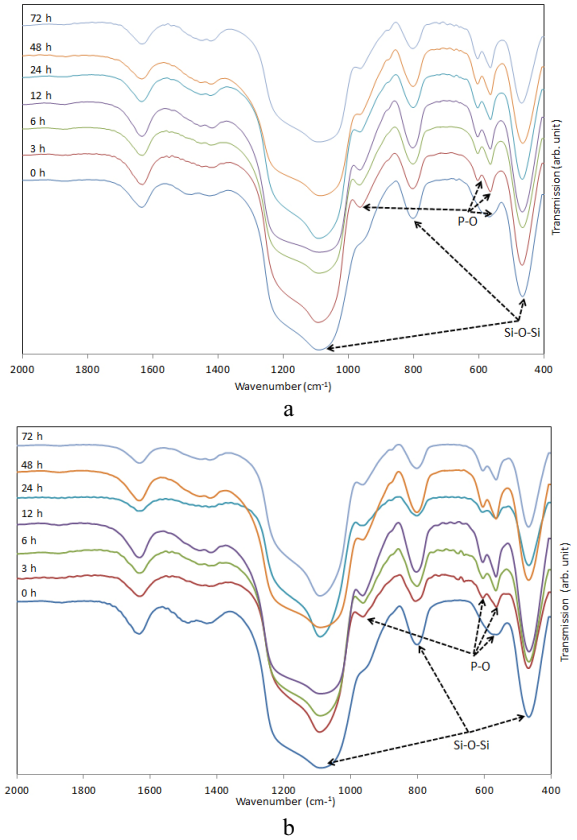

Fig. 7. Time evolution of FTIR spectra of 3DOM-BGs aged for 24 h (a) and 72 h (b), after soaking in SBF solutions for 0 h – 72 h

4. CONCLUSIONS

3DOM-BG scaffolds were synthesized by the sol-gel method using spherical PMMA colloidal crystals of 350 nm in diameter and non-ionic block copolymers P123 as cotemplates. The variation in ageing time from (0 – 72) h affected the wall thickness and windows interconnecting macropores network. The wall thickness was increased by with an increase in ageing time up to 24 h and then gradually reduced after prolonged aging. The *in vitro* bioactivity testing by soaking 3DOM-BGs in simulated body fluid at 37 °C showed the rapid formation of bone-like apatite phase, hydroxyapatite within 3 h. These results were supported by FESEM, XRD and FTIR analysis. Moreover, all results showed that the 3DOM-BG aged for 24 h had more bioactivity than those using other ageing periods.

Acknowledgments

This first author has received Ph.D. scholarship from Walailak University (Grant no. WU55609).

REFERENCES

1. **Hench, L. L.** The Story of Bioglass® *Journal of Materials Science: Materials in Medicine* 17 2006: pp. 967 – 978. http://dx.doi.org/10.1007/s10856-006-0432-z
2. **Jones, J. R.** Review of Bioactive Glass: From Hench to Hybrids. Review *Acta Biomaterialia* 9 2013: pp. 4457 – 4486. http://dx.doi.org/10.1016/j.actbio.2012.08.023
3. **Chen, Q., Larismaa, J., Keski-Honkola, A., Vilonen, K., Soderberg, O., Hannula, S.-P.** Effect of Synthesis Time on Morphology of Hollow Porous Silica Microspheres *Materials Science* (*Medžiagotyra*) 18 2012: pp. 66 – 71.
4. **Gatelyte, A., Jasaitis, D., Beganskiene, A., Kareiva, A.** Sol-gel Synthesis and Characterization of Selected Transition Metal Nano-ferrites *Materials Science* (*Medžiagotyra*) 17 2011: pp. 302 – 307.
5. **Arcos, D., Vallet-Regí, M.** Sol-gel Silica-based Biomaterials and Bone Tissue Regeneration. Review *Acta Biomaterialia* 6 2010: pp. 2874 – 2888. http://dx.doi.org/10.1016/j.actbio.2010.02.012
6. **Chen, Q. Z., Li, Y., Jin, L. Y., Quinn, J. M. W., Komesaroff, P. A.** A New Sol-gel Process for Producing Na_2O-containing Bioactive Glass Ceramics *Acta Biomaterialia* 6 2010: pp. 4143 – 4153. http://dx.doi.org/10.1016/j.actbio.2010.04.022
7. **Ma, J., Chen, C. Z., Wang, D. G., Shi, J. Z.** Textural and Structural Studies of Sol-gel Derived SiO_2–CaO– P_2O_5–MgO Glasses by Substitution of MgO for CaO *Materials Science and Engineering C* 30 2010: pp. 886 – 890. http://dx.doi.org/10.1016/j.msec.2010.04.005
8. **Lucas-Girot, A., Mezahi, F. Z., Mami, M., Oudadesse, H., Harabi, A., Floch, M. L.** Sol-gel Synthesis of a New Composition of Bioactive Glass in the Quaternary System SiO_2–CaO–Na_2O–P_2O_5 Comparison with Melting Method *Journal of Non-Crystalline Solids* 357 2011: pp. 3322 – 3327.
9. **Cacciotti, I., Lombardi, M., Bianco, A., Ravaglioli, A., Montanaro, L.,** Sol-gel Derived 45S5 Bioglass: Synthesis, Microstructural Evolution and Thermal Behavior *Journal of Materials Science: Materials in Medicine* 23 2012: pp. 1849 – 1866.

10. **Wu, C., Chang, J.** Mesoporous Bioactive Glasses: Structure Characteristics, Drug/growth Factor Delivery and Bone Regeneration Application. Review *Interface Focus* 2 2012: pp. 292 – 306. http://dx.doi.org/10.1098/rsfs.2011.0121

11. **Martin, R. A., Yue, S., Hanna, J. V., Lee, P. D., Newport, R. J., Smith, M. E., Jones, J. R.** Characterizing the Hierarchical Structures of Bioactive Sol-gel Silicate Glass and Hybrid Scaffolds for Bone Regeneration *Philosophical Transactions of the Royal Society A* 370 2012: pp. 1422 – 1443.

12. **Jones, J. R., Lin, S., Yue, S., Lee, P. D., Hanna, J. V., Smith, M. E., Newport, R. J.,** Bioactive Glass Scaffolds for Bone Regeneration and Their Hierarchical Characterization *Proceedings of the Institution of Mechanical Engineers, Part H: Journal of Engineering in Medicine* 224 2010: pp. 1373 – 1387. http://dx.doi.org/10.1243/09544119JEIM836

13. **Hung, D., Liu, Z., Shah, N., Hao, Y., Searson, P. C.** Finite Size Effects in Ordered Macroporous Electrodes Fabricated by Electrodeposition into Colloidal Crystal Templates *Journal of Physical Chemistry* 111 2007: pp. 3308 – 3313. http://dx.doi.org/10.1039/b003147j

14. **Yan, H., Blanford, C. F., Smyrlb, W. H., Stein, A.** Preparation and Structure of 3D Ordered Macroporous Alloys by PMMA Colloidal Crystal Templating *Chemistry Communications* 16 2000: pp. 1477 – 1478.

15. **Hyodo, T., Sasahara, K., Shimizu, Y., Egashira,M.** Preparation of Macroporous SnO_2 Films Using PMMA Microspheres and Their Sensing Properties to NO_x and H_2 *Sensors and Actuators B* 106 2005: pp. 580 – 590. http://dx.doi.org/10.1016/j.snb.2004.07.024

16. **Martin, G. E., Garofalini, S. H.** Sol-gel Polymerization: Analysis of Molecular Mechanisms and the Effect of Hydrogen *Journal of Non-Crystalline Solids* 171 1994: pp. 68 – 79.

17. **Kokubo, T., Takadama, H.** How Useful is SBF in Predicting *in vivo* Bone Bioactivity? *Biomaterials* 27 2006: pp. 2907 – 2915. http://dx.doi.org/10.1016/j.biomaterials.2006.01.017

18. **Zhu, Y., Wu, C., Ramaswamy, Y., Kockrick, E., Simon, P., Kaskel, S., Zreiqat, H.** Preparation, Characterization and *in vitro* Bioactivity of Mesoporous Bioactive Glasses (MBGs) Scaffolds for Bone Tissue Engineering *Microporous and Mesoporous Materials* 112 2008: pp. 494 – 503. http://dx.doi.org/10.1016/j.micromeso.2007.10.029

19. **Zhu, Y., Kaskel, S.** Comparison of the *in vitro* Bioactivity and Drug Release Property of Mesoporous Bioactive Glasses (MBGs) and Bioactive Glasses (BGs) Scaffolds *Microporous and Mesoporous Materials* 118 2009: pp. 176 – 182. http://dx.doi.org/10.1016/j.micromeso.2008.08.046

20. **Boonyang, U., Li, F., Stein, A.** Hierarchical Structure and Shaped Particles of Bioactive Glass and Its *in vitro* Bioactivity *Journal of Nanomaterials* 2013, ID 681391.

21. **Balamurugan, A., Sockalingum, G., Michel, J., Faure, J., Banchet, V., Wortham, L., Bouthors, S., Laurent-Maquin, D., Balossier, G.** Synthesis and Characterization of Sol-gel Derived Bioactive Glass for Biomedical Applications *Materials Letters* 60 2006: pp. 3752 – 3757.

22. **Stein, A., Li, F., Denny, N. R.** Morphological Control in Colloidal Crystal Templating of Inverse Opals, Hierarchical Structures, and Shaped Particles *Chemistry of Materials* 20 2008: pp. 649 – 666.

23. **Wang, D., Lin, H., Jiang, J., Han, X., Guo, W., Wu, X., Jin, Y., Qu, F.** One-pot Synthesis of Magnetic, Macro/mesoporous Bioactive Glasses for Bone Tissue Engineering *Science and Technology of Advanced Materials* 14 2013: 025004 (9 p.).